Supporting Information for

Effect of solvent motions on the dynamics of the Diels-Alder reaction

Xiaoyong Zhang,*[a] Pierre-Louis Lefebvre,[a,b] Jeremy N. Harvey*[a]

[a]Department of Chemistry, KU Leuven, Celestijnenlaan 200F, B-3001
Leuven, Belgium

[b]Quantum Theory Project,Departments of Chemistry and Physics, University
of Florida, Gainesville, Florida 32611, United States

Contents

1. EVB Potential Fitting and Performance

The parameters (A, r^0, σ in $H_{ij} (i \neq j)$, and ε_i) in the EVB potential were fitted to reproduce the M06-2X energies of structures collected from the 2D relaxed scan (**Figure** S1), by using the nonlinear least-squares (NLLS) Levenberg-Marquardt algorithm as implemented in the python SciPy library. The final set of parameters as used in the EVB simulations are listed in **Table** S1. The bonded and non-bonded force field parameters of the radical carbon (absent in the original MM3 force field) in the diradical state was set to be the same as for a standard sp^2 carbon type.

Figure S2 shows the M06-2X and EVB-determined reaction profile from reactant to product. The reaction starts with the *trans-to-cis* isomerization of the butadiene from complex RC1 to RC2 (which has a small barrier that has not been studied here), followed by cycloaddition *via* the TS to give the product (P). The EVB potential predicted a reaction barrier of 18.9 kcal/mol above the reactant complex, and a reaction energy of −38.2 kcal/mol, which are in reasonable agreement with the M06-2X/6-311+G** (21.6 and −40.2 kcal/mol, respectively) and CCSD(T)-F12 values (23.6 and −38.0 kcal/mol, respectively, based on the DFT optimized structures). Geometry optimization on the EVB PES preserves the good agreement with DFT. For example, the obtained structures of the TS are almost the same. It has been proposed that the reaction progress of the symmetrical DA reaction could be well described in terms of a reaction coordinate given by the sum of the distances corresponding to the two forming bonds (referred to as q_{RC}).[1–4] By utilizing our parameterized EVB potential as well as M06-2X, one-dimensional relaxed scans along this reaction coordinate were obtained, and the results are shown in **Figure** 1b. The reactive EVB potential is found to be able to reasonably reproduce the DFT-determined minimum energy pathway (MEP) of the reaction with butadiene and ethene, and the general nature of the change in geometrical parameters along the reaction coordinate (**Figure** S3), though it should be noted that the EVB predicts a more abrupt change in the length of the non-reactive C—C (a—b and d—e) bonds along the reaction. Nevertheless, the good general agreement indicates that the parameterized EVB potential could serve as an accurate and reliable method to study the Diels-Alder reaction in solution.

2. Grote-Hynes Theory

Aside from the nonadiabatic regime limiting case, there are some other cases in GH theory, such as the polarization caging regime, and the Kramers regime. The polarization caging regime describes a situation in which the solvent instantaneously traps the solute in a polarization cage ($\omega_{b,na}^2$ becomes negative) owing to the very large initial friction $\zeta(t = 0)$. The reaction has to wait for the solvent motions to relax the well. In this regime, solvent motions are very important, and the environment relaxation time determines the TS passage. This is essentially a limiting case of the nonadiabatic regime.

If solvent has a rapid response while reaction is rather slow, the friction kernel can be treated as a delta function at zero-frequency, and the friction is effective instantaneously. As a result, $\hat{\zeta}(\omega_r)$ becomes frequency-independent and reduces to the friction constant ξ. Then, GH theory enters the Kramers regime, and one thereby can assume that all the friction is exerted on the reaction coordinate during the TS passage. The equation to solve the reactive frequency becomes,

$$\xi = \int_0^\infty \zeta(t)dt \#(S1)$$

$$\omega_{KR}^2 - \omega_{b,eq}^2 + \omega_{KR}\xi = 0 \#(S2)$$

Solving eqn (S2) gives the reactive frequency ω_{KR}. The resulting transmission coefficient k_{KR} resembles the one obtained from Kramers theory, i.e, eqn (S4).

$$\omega_{KR} = \sqrt{\omega_{b,eq}^2 + \left(\frac{\xi}{2}\right)^2} - \frac{\xi}{2} \#(S3)$$

$$\kappa_{KR} = \frac{\omega_{KR}}{\omega_{eq}} = \sqrt{1 + \left(\frac{\xi}{2\omega_{b.eq}}\right)^2} - \frac{\xi}{2\omega_{b.eq}} \#(S4)$$

3. Figures and Tables
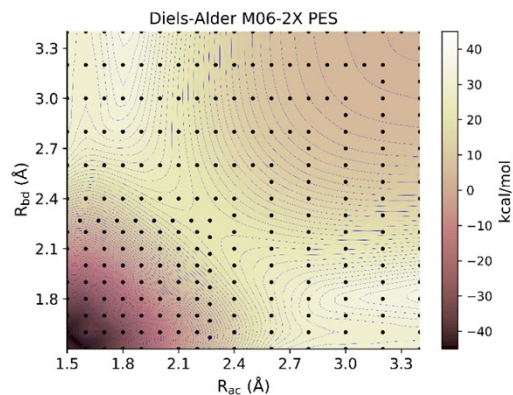
Figure S1.   Contour plot of the M06-2X/6-311+G** PES for the parent DA reactions.
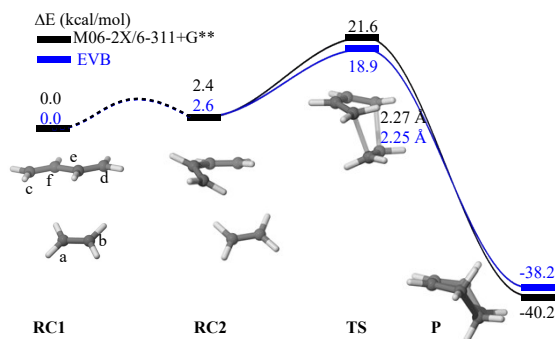
Figure S2.   Reaction profile of the DA reaction predicted by DFT (M06-2X/6-311+G**) method and the newly parameterized four-state EVB potential.

Table S1. Fitted parameters in the four-state reactive EVB potential.

	Unit	Value		Unit	Value
A_{12}	kcal/mol	57.1	σ_{23}, σ_{24}	Å	0.55
r_{12}^0	Å	4.2	ε_1	kcal/mol	-4.5
σ_{12}	Å	0.38	ε_2	kcal/mol	-51.4
A_{23}, A_{24}	kcal/mol	197.5	ε_3	kcal/mol	-5.1

| r_{23}^0, r_{24}^0 | Å | 0.87 | ε_4 | kcal/mol | -5.1 |
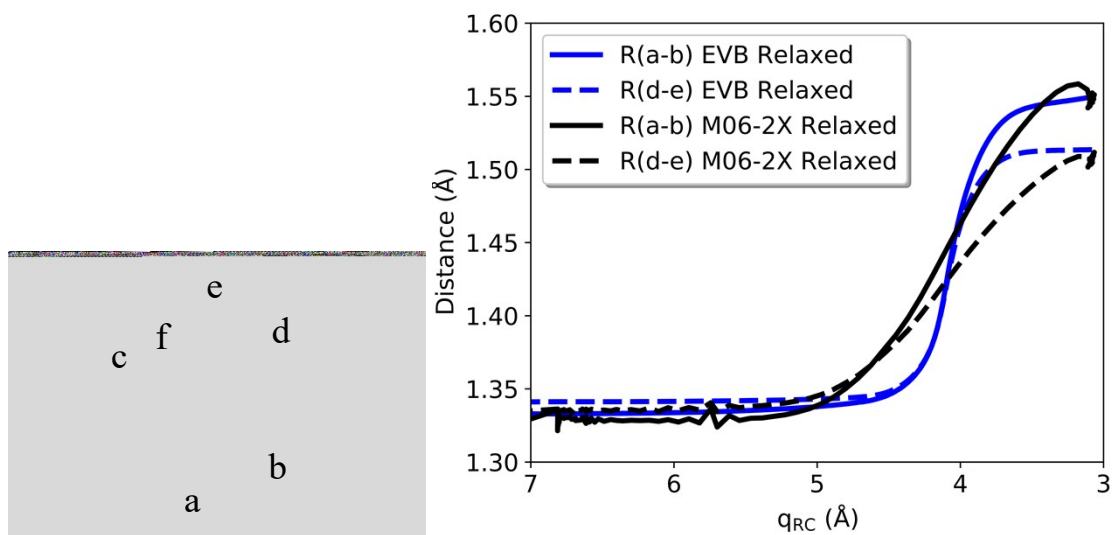
Figure S3. Variations of some geometric parameters along the reaction coordinate ($R_{ac} + R_{bd}$) of the DA reaction as predicted by the four-state EVB potential (in blue) and the M06-2X/6-311+G** (in black) method. The C-C bond distance R_{ab} of the ethene fragment is shown as a solid line, while the C-C bond distance R_{de} of butadiene is shown as a dashed line.
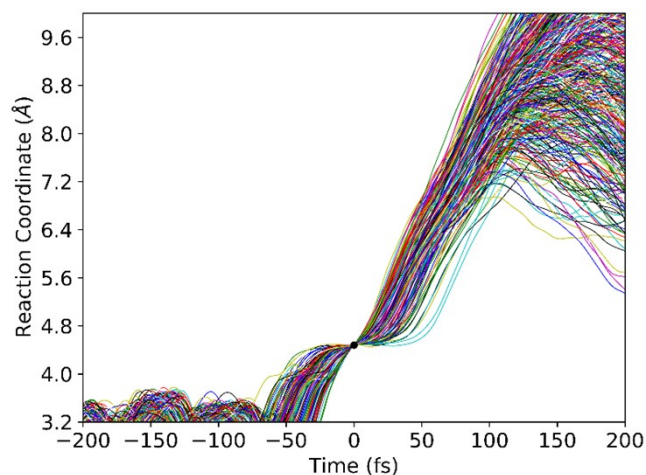
Figure S4. Evolution of the reaction coordinate with time in the reactive classical trajectory simulations of the DA reaction in the standard mass solution phase as modelled with the four-state EVB potential. **During the trajectory simulation, the solvent molecules are fixed at their initial position at time zero and not allowed to move**. Time zero is defined as being the point where the reaction coordinate lies within the dividing surface; times smaller than zero are those where

the trajectory moves towards the product side, while time greater than zero means the portion of the trajectory in the direction of the reactant side of the normal DA reaction. Note that recrossing trajectories are not plotted here.

Table S2. Number (N_{rx}) of reactive trajectories and average transit time in femtoseconds for different simulation systems. The transit time t_R and t_P is defined as the time (fs) for the reaction coordinate to change from its value at the maximum of the PMF to thresholds indicating entry into one of the potential wells: reactants for $q_{RC} > 5.8$ Å or product for $q_{RC} < 3.4$ Å, respectively.

	N_{rx}	t_R (fs)	t_P (fs)
Gas	562	40.1	38.9
^{1m}Propane	559	40.8	40.0
Propane[a]	559	40.8	40.1
^{10m}Propane	540	39.9	41.2
^{50m}Propane	544	40.8	41.2

[a] Solvent motions are frozen throughout the simulation

Table S3. The maximum number (N_{SCF}) of SCF cycles required to achieve convergence during the PMF simulations for different solution systems.

	N_{SCF}
Gas[b]	12
^{1m}Propane[b]	21
^{10m}Propane[b]	23
^{10m}Propane[a]	>100
^{50m}Propane[b]	23

a. The solute H adopts the standard value. SCF fails within 100 cycles and the total energy of system diverges.
b. The solute H mass is three time the standard value.
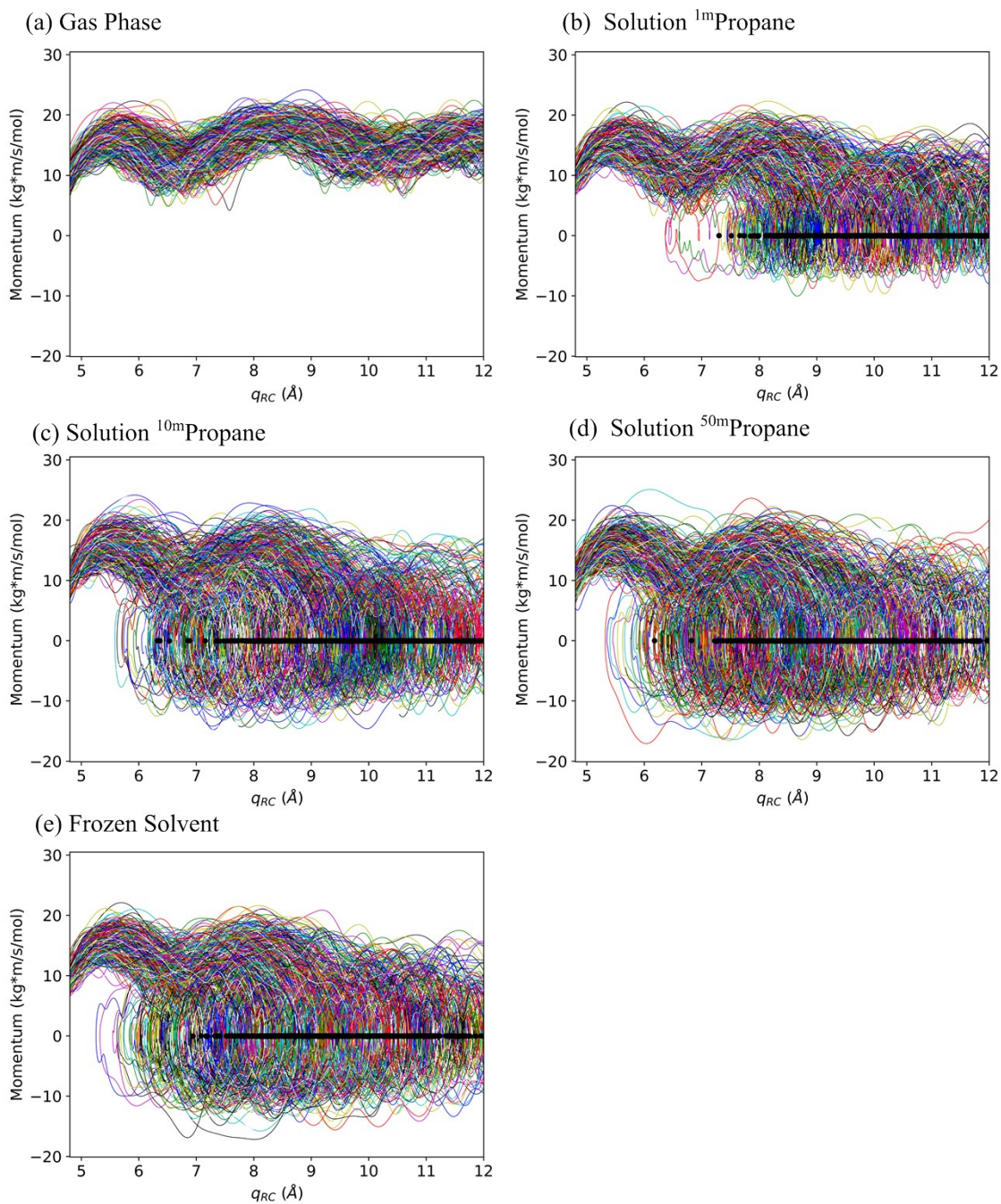
Figure S5. Momentum along the reaction coordinate in the direction leading to the reactant complex in different simulation systems for the reactive trajectories. The black dots highlight the time point in each trajectory at which the momentum for the first time is equal to zero after exiting the transition state.

7
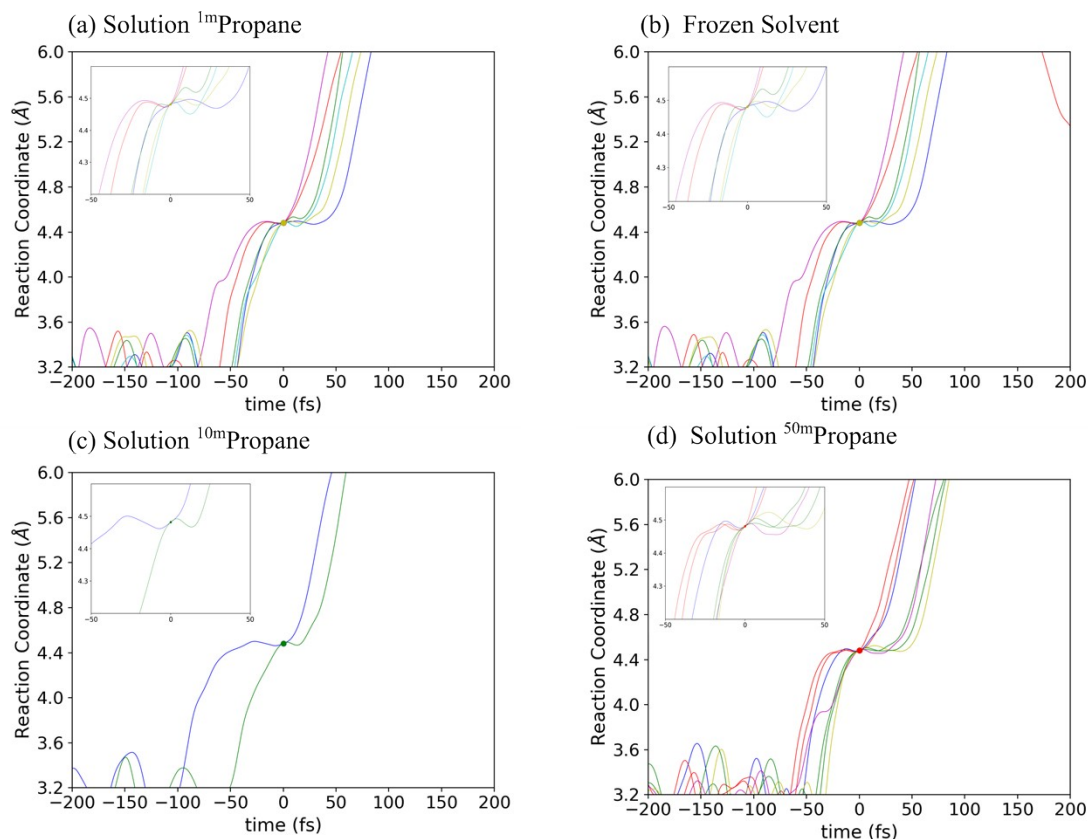
Figure S6. Reactive trajectories with recrossing behaviors for different systems.

4. References

1   J. Chandrasekhar, S. Shariffskul and W. L. Jorgensen, QM/MM simulations for Diels-Alder reactions in water: Contribution of enhanced hydrogen bonding at the transition state to the solvent effect, *J. Phys. Chem. B*, 2002, **106**, 8078–8085.

2   P. Li, F. Liu, X. Jia, Y. Shao, W. Hu, J. Zheng and Y. Mei, Efficient computation of free energy surfaces of diels–alder reactions in explicit solvent at ab initio QM/MM level, *Molecules*, 2018, **23**, 2487.

3   K. Black, P. Liu, L. Xu, C. Doubleday and K. N. Houk, Dynamics, transition states, and timing of bond formation in Diels-Alder reactions, *Proc. Natl. Acad. Sci. U. S. A.*, 2012, **109**, 12860–12865.

4   O. Acevedo and W. L. Jorgensen, Understanding rate accelerations for Diels-Alder

reactions in solution using enhanced QM/MM methodology, *J. Chem. Theory Comput.*, 2007, **3**, 1412–1419.